



***J/ψ* and D^0 production in $\sqrt{s_{NN}} = 68.5$ GeV PbNe collisions**

LHCb Collaboration*

CERN, 1211 Geneva 23, Switzerland

Received: 23 November 2022 / Accepted: 28 May 2023 / Published online: 25 July 2023
© CERN for the benefit of the LHCb collaboration 2023

Abstract The first measurement of J/ψ and D^0 production in PbNe collisions by the LHCb experiment in its fixed-target configuration is reported. The production of J/ψ and D^0 mesons is studied with a beam of lead ions with an energy of 2.5 TeV per nucleon colliding on gaseous neon targets at rest, corresponding to a nucleon-nucleon centre-of-mass energy of $\sqrt{s_{NN}} = 68.5$ GeV. The $J/\psi/D^0$ production cross-section ratio is studied as a function of rapidity, transverse momentum and collision centrality. These data are compared with measurements from $p\text{Ne}$ collisions at the same energy and show no difference in the observed J/ψ suppression trend when comparing $p\text{Ne}$ and PbNe peripheral collisions with PbNe central collisions.

In the high-density and high-temperature regime of quantum chromodynamics (QCD), the production of heavy quarks in nucleus-nucleus interactions is well suited to study the transition between ordinary hadronic matter and the hot and dense quark-gluon plasma (QGP). Since heavy quark masses are large compared to the QGP critical temperature, $T_c \sim 156$ MeV [1], their production occurs in primary nucleon-nucleon collisions, at an early stage of the interaction. They can therefore experience the full evolution of the created nuclear medium. Moreover, at sufficiently high temperature, larger than T_c , lattice QCD calculations predict that the production of charmonium ($c\bar{c}$ bound states) decreases with respect to the overall $c\bar{c}$ production, due to the modification of their binding mechanism [2]. Consequently, the proper interpretation of the charmonium suppression, observed in nucleus-nucleus collisions at various energies [3,4], requires the measurement of charmonium yields together with the overall charm quark production [5]. Since most of the charm quarks hadronise into open charm D^0 mesons, the D^0 production yield should provide a suitable reference for the study of the charmonium yield modification, assuming that D^0 production is not modified by the medium.

In this paper, the first measurement of J/ψ and D^0 production in fixed-target nucleus-nucleus collisions at the LHC is presented.¹ Lead ions with an energy per nucleon of 2.5 TeV are incident on neon nuclei at rest, corresponding to a nucleon-nucleon centre-of-mass energy of $\sqrt{s_{NN}} = 68.5$ GeV. The J/ψ and D^0 mesons are measured via their $\mu^+\mu^-$ and $K^\mp\pi^\pm$ decays, respectively.

The LHCb detector [6,7] is a single-arm forward spectrometer covering the pseudorapidity range $2 < \eta < 5$. It has been designed for the study of particles containing c or b quarks. The main detector elements are: the silicon-strip vertex locator (VELO) surrounding the interaction region that allows c and b hadrons to be identified from their characteristic flight distance; a tracking system that provides a measurement of the momentum of charged particles, with a relative uncertainty that varies from 0.5% at low momentum to 1.0% at 200 GeV; two ring-imaging Cherenkov detectors that are able to discriminate among different types of charged hadrons; a calorimeter system consisting of scintillating-pad and preshower detectors, electromagnetic and hadronic calorimeters; and a muon detector composed of alternating layers of iron and multiwire proportional chambers. The system for measuring the overlap with gas (SMOG) [8], which enables the injection of gases with pressures of $O(10^{-7})$ mbar in the beam pipe section inside the VELO, is used to operate LHCb as a fixed-target experiment. The SMOG allows the injection of noble gases and therefore gives the unique opportunity to study nucleus-nucleus and proton-nucleus collisions with various targets. Due to the boost of the centre-of-mass frame induced by the high-energy lead ion beam, the LHCb acceptance extends over the backward rapidity hemisphere in the centre-of-mass system of the reaction covering the region $-2.29 \lesssim y^* \lesssim 0$.

Selected events are recorded by a two-stage trigger system [9]. The first level is implemented in hardware and uses information provided by the calorimeters and the muon detectors,

S. Eidelman, M.-N. Minard, J. D. Roth, B. Spaan, S. Stone: Deceased.

* e-mail: fleuret@in2p3.fr

¹ The inclusion of charge-conjugate processes is implied throughout the paper.

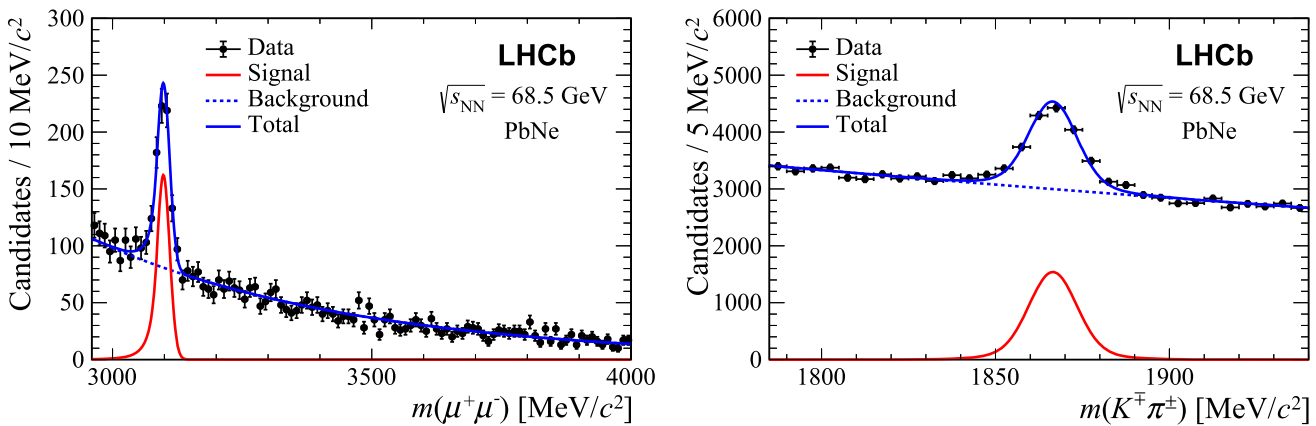


Fig. 1 Mass distributions of (left) $J/\psi \rightarrow \mu^-\mu^+$ and (right) $D^0 \rightarrow K^\mp\pi^\pm$ candidates. The data are overlaid with the fit function

while the second is a software trigger. The hardware trigger requires at least one identified muon for the selection of the $J/\psi \rightarrow \mu^+\mu^-$ decay and energy deposit in the calorimeter for the $D^0 \rightarrow K^\mp\pi^\pm$ selection. The software trigger requires two well-reconstructed muons for the J/ψ mode, while for the D^0 channel, the software trigger requires a track with transverse momentum larger than $500 \text{ MeV}/c$.

The data samples are collected under dedicated beam conditions where lead ion bunches moving towards the detector do not cross any bunch moving in the opposite direction at the nominal lead-lead (PbPb) interaction point. Events must have a reconstructed primary vertex (PV) z position (along the beam direction) within the fiducial region $z_{PV} \in [-200, 150]$ mm where high reconstruction efficiencies are achieved and calibration samples are available. In order to suppress residual PbPb collisions occurring at $z_{PV} = 0$ mm, events with activity in the backward region, with respect to the PV position, are vetoed, based on the number of hits in the VELO stations upstream of the interaction region.

The offline selection of J/ψ and D^0 candidates is similar to that used in Ref. [10]. Events must contain a primary vertex with at least four tracks reconstructed in the VELO detector. The J/ψ candidates are formed from two oppositely charged muons forming a vertex. The muons must have transverse momentum, p_T , larger than $500 \text{ MeV}/c$ and are required to be consistent with originating from the primary interaction point. Each D^0 candidate is formed from an oppositely charged pair of charged particles that come from a common displaced vertex. One of these particles must be identified as a kaon and the other as a pion. The D^0 candidates are required to have a decay time larger than 0.4 ps . The measurements are performed in the range of D^0 and J/ψ transverse momentum $p_T < 8 \text{ GeV}/c$ and rapidity $2.0 < y < 4.29$.

The kinematic acceptance and reconstruction efficiencies are determined using simulated lead-neon (PbNe) collision events. In the simulation, J/ψ and D^0 mesons are generated using PYTHIA 8 [11] with a specific LHCb configuration

[12] and with colliding lead-ion beam momenta equal to the momentum per nucleon of the beam and target in the centre-of-mass frame. Particle decays are described by EVTGEN [13], in which final-state radiation is generated using PHOTOS [14]. The four-momenta of the J/ψ and D^0 decay products are embedded into PbNe minimum bias events that are generated with the EPOS event generator [15] using beam parameters obtained from data. Decays of hadronic particles generated with EPOS are also described by EVTGEN. The interaction of the generated particles with the detector, and its response, are implemented using the GEANT4 toolkit [16, 17] as described in Ref. [18]. After reconstruction, the simulated events are assigned weights using a gradient boosted reweighter [19] to reproduce the data with respect to the multiplicity in the scintillating pad detector (denoted hereafter as hit multiplicity) and the transverse momentum distribution of the J/ψ and D^0 candidates. The overall efficiencies, including the kinematic acceptance, the efficiencies of the trigger, event selection, primary vertex reconstruction, tracking and particle identification, are 13.9% and 1.1% for the J/ψ and D^0 decays, respectively.

The J/ψ and D^0 signal yields are obtained from extended unbinned maximum-likelihood fits to their mass distributions. The J/ψ signal is described by a Crystal Ball function [20] while the D^0 signal is described by the sum of two Gaussian functions. The background components are modelled by exponential functions. Figure 1 shows the mass distribution obtained after all selection criteria are applied to the entire PbNe data set, with the fit functions superimposed. The overall yields for the J/ψ and D^0 channels are about 550 and 5700 respectively. The signal yields are determined in intervals of p_T , y^* and hit multiplicity. The yields determined from the mass fit are corrected for the geometrical acceptance of the detector and the efficiencies of the trigger, event selection, primary vertex reconstruction, tracking and particle identification. The efficiencies for particle identification [21] and tracking are obtained from a control sample of

Table 1 Summary of the systematic uncertainties affecting the $J/\psi/D^0$ production ratio. Those that are correlated between bins affect all measurements by the same relative amount. Ranges denote the minimum and the maximum values among the y , p_T or hit multiplicity bins

| Systematic uncertainties | $J/\psi/D^0$ |
|--|--------------|
| Correlated bin uncertainties | |
| Simulation weighting | 16.0% |
| MC-truth matching efficiency | 4.1% |
| PV efficiency | 0.3% |
| Tracking efficiency | 2.9% |
| Particle identification | 1.2% |
| Overall $J/\psi/D^0$ determination | 7.8% |
| Uncorrelated bin uncertainties | |
| Signal mass model | [1.1, 14.7]% |
| Simulation statistical error | [0.5, 1.8]% |
| Tracking calibration sample stat | < 0.1% |
| Particle identification calibration stat | [6.5, 6.9]% |
| Overall systematic uncertainty | 19.6% |

lead-proton ($\text{Pb}p$) collision data. All the other efficiencies are determined from simulation. Several sources of systematic uncertainties are considered, affecting either the determination of the signal yields or the total efficiencies. They are summarised in Table 1 separately for correlated and uncorrelated systematic uncertainties among the bins.

The contamination from residual PbPb collisions, evaluated to be 0.23%, is considered negligible in the $J/\psi/D^0$ production ratio. The fraction of signal from b -hadron decays at $\sqrt{s_{\text{NN}}} = 68.5$ GeV is estimated to be less than 0.1%, which is also considered to be negligible. The PV efficiency systematic uncertainty is determined by considering the difference between the PV efficiency computed using the J/ψ and D^0 simulations. The systematic uncertainty related to the mass fit is evaluated using alternative models for signal and background shapes that reproduce the mass shapes well. Another source of uncertainty arises from the finite size of the simulation sample used to compute the acceptances and efficiencies. Systematic uncertainties in the tracking and particle identification efficiencies are mainly related to the differences between the track multiplicity in PbNe and $\text{Pb}p$ collisions, and to the size of the $\text{Pb}p$ samples. The tracking systematic uncertainty also takes into account the difference in tracking efficiency between the data and the simulation. The MC-truth matching procedure is also tested and its inefficiency is considered a systematic uncertainty. Alternative sets of event weights are produced to evaluate the uncertainty associated with the reweighting procedure. The main variation is obtained by different random splitting of the training/testing samples and with different multiplicity input variables (such as the number of long tracks, or the multiplicity hits, or the clusters or tracks in the VELO).

The largest discrepancy between the data and simulation is in the primary vertex position distribution. This discrepancy mostly cancels in the $J/\psi/D^0$ ratio. To obtain the residual discrepancy, the difference between the overall $J/\psi/D^0$ efficiency ratio evaluated using the default weights and the same ratio computed with the alternative weights is studied with respect to the primary vertex position, leading to another systematic uncertainty affecting the weighting. These tests result in a correlated 16% systematic uncertainty to be applied in the $J/\psi/D^0$ production ratio. A last correlated systematic uncertainty of 7.8% takes into account the difference between the overall $J/\psi/D^0$ ratio, which is the average of the results integrated over y^* or p_T and multiplicity, and the individual results.

The $J/\psi/D^0$ cross-section ratio, taking into account the branching fractions, is

$$\frac{\sigma_{J/\psi}}{\sigma_{D^0}} = \frac{Y_{J/\psi \rightarrow \mu^+ \mu^-}}{\mathcal{B}_{J/\psi \rightarrow \mu^+ \mu^-} \times \varepsilon_{J/\psi}} \times \frac{\mathcal{B}_{D^0 \rightarrow K^\mp \pi^\pm} \times \varepsilon_{D^0}}{Y_{D^0 \rightarrow K^\mp \pi^\pm}} \\ = 0.51 \pm 0.04 \text{ (stat.)} \pm 0.10 \text{ (syst.)}\%,$$

where $Y_{J/\psi \rightarrow \mu^+ \mu^-}$ ($Y_{D^0 \rightarrow K^\mp \pi^\pm}$), $\mathcal{B}_{J/\psi \rightarrow \mu^+ \mu^-}$ ($\mathcal{B}_{D^0 \rightarrow K^\mp \pi^\pm}$) and $\varepsilon_{J/\psi}$ (ε_{D^0}) are J/ψ (D^0) yield, branching fraction and total efficiency, respectively. The $J/\psi/D^0$ cross-section ratio as a function of y^* and p_T is shown in Fig. 2. The ratio depends strongly on p_T but the data are compatible with no dependence on centre-of-mass rapidity.

The $J/\psi/D^0$ cross sections ratios in PbNe collision data are compared with measurements in p Ne collisions with LHCb in similar experimental conditions [22,23]. The left panel of Fig. 3 shows the $J/\psi/D^0$ cross-section ratio for both PbNe and p Ne data as a function of AB , the product of the beam (A) and target (B) atomic mass numbers. Assuming that nuclear effects, that can modify the initial $c\bar{c}$ pair production, cancel in the $J/\psi/D^0$ ratio, and that the J/ψ and D^0 production cross-sections are of the form $\sigma_{J/\psi}^{AB} = \sigma_{J/\psi}^{pp} \times AB^\alpha$ and $\sigma_{D^0}^{AB} = \sigma_{D^0}^{pp} \times AB$, respectively, the cross-section ratio dependence on AB is expected to follow

$$\frac{\sigma_{J/\psi}^{AB}}{\sigma_{D^0}^{AB}} = \frac{\sigma_{J/\psi}^{pp}}{\sigma_{D^0}^{pp}} \times (AB)^{\alpha-1} = C \times (AB)^{\alpha-1}. \quad (1)$$

A fit to the data gives $\alpha = 0.86 \pm 0.04$ (and $C = (1.59 \pm 0.26) \times 10^{-2}$), which indicates that J/ψ production is affected by additional nuclear effects with respect to D^0 production.

Figure 3 (right) also shows the $J/\psi/D^0$ cross-section ratio as a function of the number of binary nucleon-nucleon collisions, N_{coll} . The PbNe data sample is divided into intervals of N_{coll} corresponding to different centrality intervals related to the overlap region between the two colliding nuclei. The larger the N_{coll} the larger is the overlap region. Since small overlap regions correspond to small N_{coll} values (similar to

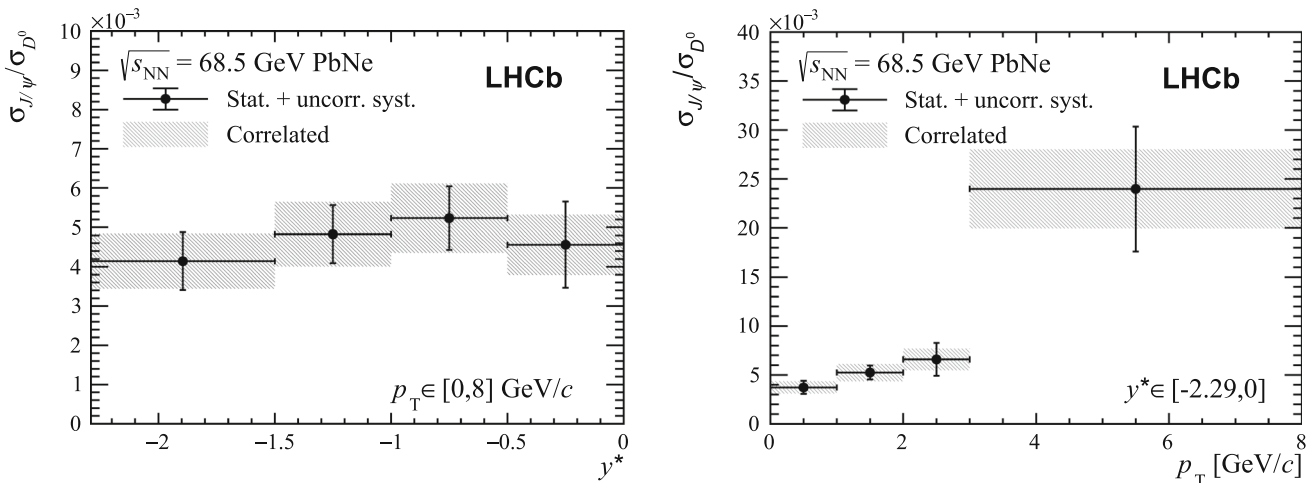


Fig. 2 Ratios of J/ψ to D^0 cross-sections as a function of (left) y^* and (right) transverse momentum. The error bars represent uncertainties that are uncorrelated bin-to-bin while the boxes represent the correlated uncertainties

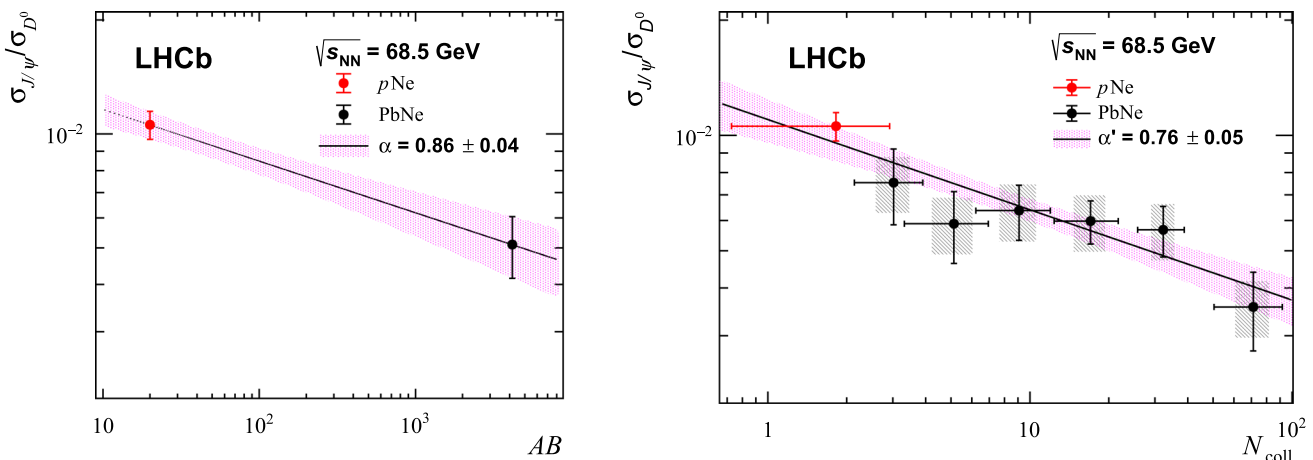


Fig. 3 Left: $J/\psi/D^0$ cross-section ratio as a function of AB , the product of the beam (A) and target (B) atomic mass numbers; the error bars represent the quadratic sum of statistical and systematic uncertainties. Right: $J/\psi/D^0$ cross-section ratio as a function of N_{coll} ; the error bars

represent the quadratic sum of statistical and uncorrelated systematic uncertainties while the boxes correspond to the correlated systematic uncertainty. The red and black points correspond to $p\text{Ne}$ [22] and PbNe collisions, respectively

N_{coll} values in proton-nucleus collisions), any suppression related to the formation of a deconfined medium should occur at large N_{coll} values.

The number of binary collisions is not directly observable but it can be mapped to the actual data using a Glauber model. In LHCb, this mapping, reported in Table 2, is performed based on the hit multiplicity, as detailed in Ref. [24]. For $p\text{Ne}$ collisions, the result is integrated over the impact parameter of the collision. Assuming that the J/ψ and D^0 production cross-sections scale as $\langle N_{\text{coll}} \rangle^{\alpha'}$ and $\langle N_{\text{coll}} \rangle$ respectively, the cross-section ratio $\sigma_{J/\psi}/\sigma_{D^0}$ scales as $\langle N_{\text{coll}} \rangle^{\alpha'-1}$. A fit to the data (where the PbNe correlated systematic uncertainty is not taken into account) gives $\alpha' = 0.76 \pm 0.05$, compatible with α when relating N_{coll} to AB with the Glauber model. This confirms that J/ψ meson production is affected

by additional nuclear effects with respect to D^0 production. Moreover, within uncertainties, no difference in the J/ψ suppression trend is observed when comparing the PbNe largest N_{coll} bin with the $p\text{Ne}$ and PbNe smaller N_{coll} bins.

In summary, we report on the J/ψ to D^0 production ratio in $\sqrt{s_{\text{NN}}} = 68.5 \text{ GeV}$ PbNe collisions with the LHCb experiment. The $J/\psi/D^0$ cross-section ratio is found to be $\sigma_{J/\psi}/\sigma_{D^0} = 0.51 \pm 0.04 \text{ (stat.)} \pm 0.10 \text{ (syst.)}\%$ for $y^* \in [-2.29, 0]$ and $p_T \in [0, 8] \text{ GeV}/c$. When compared with results obtained in $p\text{Ne}$ collisions, the dependence of this ratio with $(AB)^{\alpha-1}$ gives $\alpha = 0.86 \pm 0.04$. Finally, the study of this ratio, divided into intervals of N_{coll} , shows no difference in the J/ψ suppression trend, when comparing $p\text{Ne}$ and PbNe peripheral collisions with PbNe central collisions.

Table 2 The mapping from intervals of the hit multiplicity to intervals of N_{coll} ; $\langle N_{\text{coll}} \rangle$ and $\text{RMS}(N_{\text{coll}})$ correspond to the N_{coll} distribution mean and root mean square values respectively

| | Hit multiplicity | $\langle N_{\text{coll}} \rangle$ | $\text{RMS}(N_{\text{coll}})$ |
|-------------------------------|------------------|-----------------------------------|-------------------------------|
| $p\text{Ne}$ PbNe | 0–200 | 1.81 | 1.10 |
| | 200–300 | 3.02 | 0.88 |
| | 300–446 | 5.13 | 1.81 |
| | 446–715 | 9.09 | 2.87 |
| | 715–960 | 17.04 | 4.67 |
| | 960–1700 | 32.26 | 6.51 |
| | | 71.12 | 20.70 |

Acknowledgements We express our gratitude to our colleagues in the CERN accelerator departments for the excellent performance of the LHC. We thank the technical and administrative staff at the LHCb institutes. We acknowledge support from CERN and from the national agencies: CAPES, CNPq, FAPERJ and FINEP (Brazil); MOST and NSFC (China); CNRS/IN2P3 (France); BMBF, DFG and MPG (Germany); INFN (Italy); NWO (Netherlands); MNiSW and NCN (Poland); MEN/IFA (Romania); MICINN (Spain); SNSF and SER (Switzerland); NASU (Ukraine); STFC (United Kingdom); DOE NP and NSF (USA). We acknowledge the computing resources that are provided by CERN, IN2P3 (France), KIT and DESY (Germany), INFN (Italy), SURF (Netherlands), PIC (Spain), GridPP (United Kingdom), CSCS (Switzerland), IFIN-HH (Romania), CBPF (Brazil), Polish WLCG (Poland) and NERSC (USA). We are indebted to the communities behind the multiple open-source software packages on which we depend. Individual groups or members have received support from ARC and ARDC (Australia); Minciencias (Colombia); AvH Foundation (Germany); EPLANET, Marie Skłodowska-Curie Actions and ERC (European Union); A*MIDEX, ANR, IPhU and GLUODYNAMICS/Labex P2IO, and Région Auvergne-Rhône-Alpes (France); Key Research Program of Frontier Sciences of CAS, CAS PIFI, CAS CCEPP, Fundamental Research Funds for the Central Universities, and Sci. & Tech. Program of Guangzhou (China); GVA, XuntaGal, GENCAT and Prog. Atracción Talento, CM (Spain); SRC (Sweden); the Leverhulme Trust, the Royal Society and UKRI (United Kingdom).

Data Availability Statement This manuscript has no associated data or the data will not be deposited. [Authors' comment: Data associated to the plots in this publication are made available on the CERN document server at <https://cds.cern.ch/record/2841845>.]

Open Access This article is licensed under a Creative Commons Attribution 4.0 International License, which permits use, sharing, adaptation, distribution and reproduction in any medium or format, as long as you give appropriate credit to the original author(s) and the source, provide a link to the Creative Commons licence, and indicate if changes were made. The images or other third party material in this article are included in the article's Creative Commons licence, unless indicated otherwise in a credit line to the material. If material is not included in the article's Creative Commons licence and your intended use is not permitted by statutory regulation or exceeds the permitted use, you will need to obtain permission directly from the copyright holder. To view a copy of this licence, visit <http://creativecommons.org/licenses/by/4.0/>.

Funded by SCOAP³. SCOAP³ supports the goals of the International Year of Basic Sciences for Sustainable Development.

References

1. A. Bazarov et al., Chiral crossover in QCD at zero and non-zero chemical potentials. *Phys. Lett. B* **795**, 15 (2019). <https://doi.org/10.1016/j.physletb.2019.05.013>
2. S. Digal et al., Heavy quark interactions in finite temperature QCD. *Eur. Phys. J. C* **43**, 71 (2005). <https://doi.org/10.1140/epjc/s2005-02309-7>
3. L. Kluberg, H. Satz, Color deconfinement and charmonium production in nuclear collisions, Landolt–Börnstein–Group I Elementary Particles, Nuclei and Atoms. In: Stock, R. (ed.) Springer Materials, vol. 23 (2010). https://doi.org/10.1007/978-3-642-01539-7_13. [arXiv:0901.3831](https://arxiv.org/abs/0901.3831)
4. A. Andronic et al., Heavy-flavour and quarkonium production in the LHC era: from proton-proton to heavy-ion collisions. *Eur. Phys. J. C* **76**, 107 (2016). <https://doi.org/10.1140/epjc/s10052-015-3819-5>
5. H. Satz, K. Sridhar, Charmonium production versus open charm in nuclear collisions. *Phys. Rev. D* **50**, 3557 (1994). <https://doi.org/10.1103/PhysRevD.50.3557>
6. LHCb Collaboration, A.A. Alves Jr et al., The LHCb detector at the LHC. *JINST* **3**, S08005 (2008). <https://doi.org/10.1088/1748-0221/3/08/S08005>
7. LHCb Collaboration, R. Aaij et al., LHCb detector performance. *Int. J. Mod. Phys. A* **30**, 1530022 (2015). <https://doi.org/10.1142/S0217751X15300227>. [arXiv:1412.6352](https://arxiv.org/abs/1412.6352)
8. LHCb Collaboration, R. Aaij et al., Precision luminosity measurements at LHCb. *JINST* **9**, P12005 (2014). <https://doi.org/10.1088/1748-0221/9/12/P12005>. [arXiv:1410.0149](https://arxiv.org/abs/1410.0149)
9. LHCb Collaboration, R. Aaij et al., The LHCb trigger and its performance in 2011. *JINST* **8**, P04022 (2013). <https://doi.org/10.1088/1748-0221/8/04/P04022>. [arXiv:1211.3055](https://arxiv.org/abs/1211.3055)
10. LHCb Collaboration, R. Aaij et al., First measurement of charm production in fixed-target configuration at the LHC. *Phys. Rev. Lett.* **122**, 132002 (2019). <https://doi.org/10.1103/PhysRevLett.122.132002>. [arXiv:1810.07907](https://arxiv.org/abs/1810.07907)
11. T. Sjöstrand, S. Mrenna, P. Skands, A brief introduction to Pythia 8.1. *Comput. Phys. Commun.* **178**, 852 (2008). <https://doi.org/10.1016/j.cpc.2008.01.036>. [arXiv:0710.3820](https://arxiv.org/abs/0710.3820)
12. LHCb Collaboration, I. Belyaev et al., Handling of the generation of primary events in Gauss, the LHCb simulation framework. *J. Phys. Conf. Ser.* **331**, 032047 (2011). <https://doi.org/10.1088/1742-6596/331/3/032047>
13. D.J. Lange, The EvtGen particle decay simulation package. *Nucl. Instrum. Methods A* **462**, 152 (2001). [https://doi.org/10.1016/S0167-9002\(01\)00089-4](https://doi.org/10.1016/S0167-9002(01)00089-4)
14. P. Golonka, Z. Was, PHOTOS Monte Carlo: a precision tool for QED corrections in Z and W decays. *Eur. Phys. J. C* **45**, 97 (2006). <https://doi.org/10.1140/epjc/s2005-02396-4>
15. T. Pierog et al., EPOS LHC: test of collective hadronization with data measured at the CERN Large Hadron Collider. *Phys. Rev. C* **92**, 034906 (2015). <https://doi.org/10.1103/PhysRevC.92.034906>. [arXiv:1306.0121](https://arxiv.org/abs/1306.0121)
16. Geant4 Collaboration, J. Allison et al., Geant4 developments and applications. *IEEE Trans. Nucl. Sci.* **53**, 270 (2006). <https://doi.org/10.1109/TNS.2006.869826>
17. Geant4 Collaboration, S. Agostinelli et al., Geant4: a simulation toolkit. *Nucl. Instr. Methods* **506**, 250 (2003). [https://doi.org/10.1016/S0167-9002\(03\)01368-8](https://doi.org/10.1016/S0167-9002(03)01368-8)
18. M. Clemencic et al., The LHCb simulation application, Gauss: design, evolution and experience. *J. Phys. Conf. Ser.* **331**, 032023 (2011). <https://doi.org/10.1088/1742-6596/331/3/032023>

19. A. Rogozhnikov, Reweighting with boosted decision trees. J. Phys. Conf. Ser. **762**(1), 012036 (2016). <https://doi.org/10.1088/1742-6596/762/1/012036>. <https://github.com/arogozhnikov/hepml>. arXiv:1608.05806
20. T. Skwarnicki, A study of the radiative cascade transitions between the Upsilon-Prime and Upsilonon resonances. PhD thesis, Institute of Nuclear Physics, Krakow, DESY-F31-86-02 (1986)
21. L. Anderlini et al., The PIDCalib package, LHCb-PUB-2016-021. http://cdsweb.cern.ch/search?p=LHCb-PUB-2016-021&f=reportnumber&action_search=Search&c=LHCb+Notes
22. LHCb Collaboration, R. Aaij et al., Charmonium production in $\sqrt{s_{NN}} = 68.5\text{GeV}$ $p\text{Ne}$ collisions. Eur. Phys. J. C **83**, 625 (2023). <https://doi.org/10.1140/epjc/s10052-023-11608-6>. arXiv:2211.11645
23. LHCb Collaboration, R. Aaij et al., Open charm production and asymmetry in $p\text{Ne}$ collisions at $\sqrt{s_{NN}} = 68.5\text{GeV}$. Eur. Phys. J. C **83**, 541 (2023). <https://doi.org/10.1140/epjc/s10052-023-11641-5>. arXiv:2211.11633
24. LHCb Collaboration, R. Aaij et al., Centrality determination in heavy-ion collisions with the LHCb detector. JINST **17**, P05009 (2022). <https://doi.org/10.1088/1748-0221/17/05/P05009>. arXiv:2111.01607

LHCb Collaboration*

- R. Aaij³², A. S. W. Abdelmotteleb⁵⁰, C. Abellan Beteta⁴⁴, F. Abudinén⁵⁰, T. Ackernley⁵⁴, B. Adeva⁴⁰, M. Adinolfi⁴⁸, H. Afsharnia⁹, C. Agapopoulou¹³, C. A. Aidala⁷⁶, S. Aiola²⁵, Z. Ajaltouni⁹, S. Akar⁵⁹, K. Akiba³², J. Albrecht¹⁵, F. Alessio⁴², M. Alexander⁵³, A. Alfonso Albero³⁹, Z. Aliouche⁵⁶, P. Alvarez Cartelle⁴⁹, R. Amalric¹³, S. Amato², J. L. Amey⁴⁸, Y. Amhis^{11,42}, L. An⁴², L. Anderlini²², M. Andersson⁴⁴, A. Andreianov³⁸, M. Andreotti²¹, D. Andreou⁶², D. Ao⁶, F. Archilli¹⁷, A. Artamonov³⁸, M. Artuso⁶², E. Aslanides¹⁰, M. Atzeni⁴⁴, B. Audurier¹², S. Bachmann¹⁷, M. Bachmayer⁴³, J. J. Back⁵⁰, A. Bailly-reyre¹³, P. Baladron Rodriguez⁴⁰, V. Balagura¹², W. Baldini²¹, J. SBaptista de ouza Leite¹, M. Barbetti^{22,j}, R. J. Barlow⁵⁶, S. Barsuk¹¹, W. Barter⁵⁵, M. Bartolini⁴⁹, F. Baryshnikov³⁸, J. M. Basels¹⁴, G. Bassi^{29,q}, B. Batsukh⁴, A. Battig¹⁵, A. Bay⁴³, A. Beck⁵⁰, M. Becker¹⁵, F. Bedeschi²⁹, I. B. Bediaga¹, A. Beiter⁶², V. Belavin³⁸, S. Belin⁴⁰, V. Bellee⁴⁴, K. Belous³⁸, I. Belov³⁸, I. Belyaev³⁸, G. Benane¹⁰, G. Bencivenni²³, E. Ben-Haim¹³, A. Berezhnoy³⁸, R. Bernet⁴⁴, D. Berninghoff¹⁷, H. C. Bernstein⁶², C. Bertella⁵⁶, A. Bertolin²⁸, C. Betancourt⁴⁴, F. Betti⁴², Ia. Bezshykko⁴⁴, S. Bhasin⁴⁸, J. Bhom³⁵, L. Bian⁶⁷, M. S. Bieker¹⁵, N. V. Biesuz²¹, S. Bifani⁴⁷, P. Billoir¹³, A. Biolchini³², M. Birch⁵⁵, F. C. R. Bishop⁴⁹, A. Bitadze⁵⁶, A. Bizzeti¹⁰, M. P. Blago⁴⁹, T. Blake⁵⁰, F. Blanc⁴³, S. Blusk⁶², D. Bobulska⁵³, J. A. Boelhauve¹⁵, O. Boente Garcia¹², T. Boettcher⁵⁹, A. Boldyrev³⁸, C. S. Bolognani⁷³, N. Bondar^{38,42}, S. Borghi⁵⁶, M. Borsato¹⁷, J. T. Borsuk³⁵, S. A. Bouchiba⁴³, T. J. V. Bowcock^{42,54}, A. Boyer⁴², C. Bozzi²¹, M. J. Bradley⁵⁵, S. Braun⁶⁰, A. Brea Rodriguez⁴⁰, J. Brodzicka³⁵, A. Brossa Gonzalo⁵⁰, D. Brundu²⁷, A. Buonauro⁴⁴, L. Buonincontri²⁸, A. T. Burke⁵⁶, C. Burri⁴², A. Bursche⁶⁶, A. Butkevich³⁸, J. S. Butter³², J. Buytaert⁴², W. Byczynski⁴², S. Cadeddu²⁷, H. Cai⁶⁷, R. Calabrese^{21,i}, L. Calefice^{13,15}, S. Cali²³, R. Calladine⁴⁷, M. Calvi^{26,m}, M. Calvo Gomez⁷⁴, P. Camargo Magalhaes⁴⁸, P. Campana²³, D. H. Campora Perez⁷³, A. F. Campoverde Quezada⁶, S. Capelli^{26,m}, L. Capriotti^{20,g}, A. Carbone^{20,g}, G. Carboni³¹, R. Cardinale^{24,k}, A. Cardini²⁷, I. Carli⁴, P. Carniti^{26,m}, L. Carus¹⁴, A. Casais Vidal⁴⁰, R. Caspary¹⁷, G. Casse⁵⁴, M. Cattaneo⁴², G. Cavallero⁴², V. Cavallini^{21,i}, S. Celani⁴³, J. Cerasoli¹⁰, D. Cervenkov⁵⁷, A. J. Chadwick⁵⁴, M. G. Chapman⁴⁸, M. Charles¹³, Ph. Charpentier⁴², C. A. Chavez Barajas⁵⁴, M. Chefdeville⁸, C. Chen³, S. Chen⁴, A. Chernov³⁵, S. Chernyshenko⁴⁶, V. Chobanova⁴⁰, S. Cholak⁴³, M. Chrzaszcz³⁵, A. Chubykin³⁸, V. Chulikov³⁸, P. Ciambrone²³, M. F. Cicala⁵⁰, X. Cid Vidal⁴⁰, G. Ciezarek⁴², G. Ciullo^{21,i}, P. E. L. Clarke⁵², M. Clemencic⁴², H. V. Cliff⁴⁹, J. Closier⁴², J. L. Cobbley⁵⁶, V. Coco⁴², J. A. B. Coelho¹¹, J. Cogan¹⁰, E. Cogneras⁹, L. Cojocariu³⁷, P. Collins⁴², T. Colombo⁴², L. Congedo¹⁹, A. Contu²⁷, N. Cooke⁴⁷, G. Coombs⁵³, I. Corredoira⁴⁰, G. Corti⁴², B. Couturier⁴², D. C. Craik⁵⁸, J. Crkovská⁶¹, M. Cruz Torres^{1,e}, R. Currie⁵², C. L. Da Silva⁶¹, S. Dadabaev³⁸, L. Dai⁶⁵, E. Dall'Occo¹⁵, J. Dalseno⁴⁰, C. D'Ambrosio⁴², A. Danilina³⁸, P. d'Argent¹⁵, J. E. Davies⁵⁶, A. Davis⁵⁶, O. De Aguiar Francisco⁵⁶, J. de Boer⁴², K. De Bruyn⁷², S. De Capua⁵⁶, M. De Cian⁴³, U. De Freitas Carneiro Da Graca¹, E. De Lucia²³, J. M. De Miranda¹, L. De Paula², M. De Serio^{19,f}, D. De Simone⁴⁴, P. De Simone²³, F. De Vellis¹⁵, J. A. de Vries⁷³, C. T. Dean⁶¹, F. Debernardis^{19,f}, D. Decamp⁸, V. Dedu¹⁰, L. Del Buono¹³, B. Delaney⁵⁸, H.-P. Dembinski¹⁵, V. Denysenko⁴⁴, O. Deschamps⁹, F. Dettori^{27,h}, B. Dey⁷⁰, A. Di Cicco²³, P. Di Nezza²³, I. Diachkov³⁸, S. Didenko³⁸, L. Dieste Maronas⁴⁰, S. Ding⁶², V. Dobishuk⁴⁶, A. Dolmatov³⁸<img alt="ORCID

- V. Egorychev³⁸, S. Eidelman^{38,*}, S. Eisenhardt⁵², S. Ek-In⁴³, L. Eklund⁷⁵, S. Ely⁶², A. Ene³⁷, E. Epple⁶¹, S. Escher¹⁴, J. Eschle⁴⁴, S. Esen⁴⁴, T. Evans⁵⁶, L. N. Falcao¹, Y. Fan⁶, B. Fang⁶⁷, S. Farry⁵⁴, D. Fazzini^{26,m}, M. Feo⁴², A. D. Fernez⁶⁰, F. Ferrari²⁰, L. Ferreira Lopes⁴³, F. Ferreira Rodrigues², S. Ferreres Sole³², M. Ferrillo⁴⁴, M. Ferro-Luzzi⁴², S. Filippov³⁸, R. A. Fini¹⁹, M. Fiorini^{21,i}, M. Firlej³⁴, K. M. Fischer⁵⁷, D. S. Fitzgerald⁷⁶, C. Fitzpatrick⁵⁶, T. Fiutowski³⁴, F. Fleuret¹², M. Fontana¹³, F. Fontanelli^{24,k}, R. Forty⁴², D. Foulds-Holt⁴⁹, V. Franco Lima⁵⁴, M. Franco Sevilla⁶⁰, M. Frank⁴², E. Franzoso^{21,i}, G. Frau¹⁷, C. Frei⁴², D. A. Friday⁵³, J. Fu⁶, Q. Fuehring¹⁵, E. Gabriel³², G. Galati^{19,f}, M. D. Galati⁷², A. Gallas Torreira⁴⁰, D. Galli^{20,g}, S. Gambetta^{42,52}, Y. Gan³, M. Gandelman², P. Gandini²⁵, Y. Gao⁵, M. Garau^{27,h}, L. M. Garcia Martin⁵⁰, P. Garcia Moreno³⁹, J. Garcia Pardiñas^{26,m}, B. Garcia Plana⁴⁰, F. A. Garcia Rosales¹², L. Garrido³⁹, C. Gaspar⁴², R. E. Geertsema³², D. Gerick¹⁷, L. L. Gerken¹⁵, E. Gersabeck⁵⁶, M. Gersabeck⁵⁶, T. Gershon⁵⁰, L. Giambastiani²⁸, V. Gibson⁴⁹, H. K. Giemza³⁶, A. L. Gilman⁵⁷, M. Giovannetti^{23,t}, A. Gioventù⁴⁰, P. Gironella Gironell³⁹, C. Giugliano^{21,i}, M. A. Giza³⁵, K. Gizzdov⁵², E. L. Gkougkousis⁴², V. V. Gligorov^{13,42}, C. Göbel⁶⁴, E. Golobardes⁷⁴, D. Golubkov³⁸, A. Golutvin^{55,38}, A. Gomes^{1,a}, S. Gomez Fernandez³⁹, F. Goncalves Abrantes⁵⁷, M. Goncerz³⁵, G. Gong³, I. V. Gorelov³⁸, C. Gotti²⁰, J. P. Grabowski¹⁷, T. Grammatico¹³, L. A. Granado Cardoso⁴², E. Graugés³⁹, E. Graverini⁴³, G. Graziani¹, A. T. Grecu³⁷, L. M. Greeven³², N. A. Grieser⁴, L. Grillo⁵³, S. Gromov³⁸, B. R. Gruberg Cazon⁵⁷, C. Gu³, M. Guarise^{21,i}, M. Guittiere¹¹, P. A. Günther¹⁷, E. Gushchin³⁸, A. Guth¹⁴, Y. Guz³⁸, T. Gys⁴², T. Hadavizadeh⁶³, G. Haefeli⁴³, C. Haen⁴², J. Haimberger⁴², S. C. Haines⁴⁹, T. Halewood-leagas⁵⁴, M. M. Halvorsen⁴², P. M. Hamilton⁶⁰, J. Hammerich⁵⁴, Q. Han⁷, X. Han¹⁷, E. B. Hansen⁵⁶, S. Hansmann-Menzemer^{17,42}, L. Hao⁶, N. Harnew⁵⁷, T. Harrison⁵⁴, C. Hasse⁴², M. Hatch⁴², J. He^{6,c}, K. Heijhoff³², K. Heinicke¹⁵, C. Henderson⁵⁹, R. D. L. Henderson^{63,50}, A. M. Hennequin⁵⁸, K. Hennessee⁵⁴, L. Henry⁴², J. Heuel¹⁴, A. Hicheur², D. Hill⁴³, M. Hilton⁵⁶, S. E. Hollitt¹⁵, R. Hou⁷, Y. Hou⁸, J. Hu¹⁷, J. Hu⁶⁶, W. Hu⁵, X. Hu³, W. Huang⁶, X. Huang⁶⁷, W. Hulsbergen³², R. J. Hunter⁵⁰, M. Hushchyn³⁸, D. Hutchcroft⁵⁴, P. Ibis¹⁵, M. Idzik³⁴, D. Iljin³⁸, P. Ilten⁵⁹, A. Inglessi³⁸, A. Inuiukhin³⁸, A. Ishteev³⁸, K. Ivshin³⁸, R. Jacobsson⁴², H. Jage¹⁴, S. J. Jaimes Elles⁴¹, S. Jakobsen⁴², E. Jans³², B. K. Jashal⁴¹, A. Jawahery⁶⁰, V. Jevtic¹⁵, X. Jiang^{4,6}, Y. Jiang⁶, M. John⁵⁷, D. Johnson⁵⁸, C. R. Jones⁴⁹, T. P. Jones⁵⁰, B. Jost⁴², N. Jurik⁴², I. Juszczak³⁵, S. Kandybei⁴⁵, Y. Kang³, M. Karacson⁴², D. Karpenkov³⁸, M. Karpov³⁸, J. W. Kautz⁵⁹, F. Keizer⁴², D. M. Keller⁶², M. Kenzie⁵⁰, T. Ketel³³, B. Khanji¹⁵, A. Kharisova³⁸, S. Khodenko³⁸, T. Kirn¹⁴, V. S. Kirsebom⁴³, O. Kitouni⁵⁸, S. Klaver³³, N. Kleijne^{29,q}, K. Klimaszewski³⁶, M. R. Kmiec³⁶, S. Koliev⁴⁶, A. Kondybayeva³⁸, A. Konoplyannikov³⁸, P. Kopciewicz³⁴, R. Kopecna¹⁷, P. Koppenburg³², M. Korolev³⁸, I. Kostiuk^{32,46}, O. Kot⁴⁶, S. Kotriakhova¹, A. Kozachuk³⁸, P. Kravchenko³⁸, L. Kravchuk³⁸, R. D. Krawczyk⁴², M. Kreps⁵⁰, S. Kretzschmar¹⁴, P. Krokovny³⁸, W. Krupa³⁴, W. Krzemien³⁶, J. Kubat¹⁷, W. Kucewicz^{34,35}, M. Kucharczyk³⁵, V. Kudryavtsev³⁸, G. J. Kunde⁶¹, A. Kups⁷⁵, D. Lacarrere⁴², G. Lafferty⁵⁶, A. Lai²⁷, A. Lampis^{27,h}, D. Lancierini⁴⁴, J. J. Lane⁵⁶, R. Lane⁴⁸, G. Lanfranchi²³, C. Langenbruch¹⁴, J. Langer¹⁵, O. Lantwin³⁸, T. Latham⁵⁰, F. Lazzari^{29,u}, M. Lazzaroni^{25,l}, R. Le Gac¹⁰, S. H. Lee⁷⁶, R. Lefèvre⁹, A. Leflat³⁸, S. Legotin³⁸, P. Lenisa^{21,i}, O. Leroy¹⁰, T. Lesiak³⁵, B. Leverington¹⁷, A. Li³, H. Li⁶⁶, K. Li⁷, P. Li¹⁷, S. Li⁷, T. Li⁶⁶, Y. Li⁴, Z. Li⁶², X. Liang⁶², C. Lin⁶, T. Lin⁵¹, R. Lindner⁴², V. Lisovskyi¹⁵, R. Litvinov^{27,h}, G. Liu⁶⁶, H. Liu⁶, Q. Liu⁶, S. Liu^{4,6}, A. Lobo Salvia³⁹, A. Loi²⁷, R. Lollini⁷¹, J. Lomba Castro⁴⁰, I. Longstaff⁵³, J. H. Lopes², S. L. López Soliño⁴⁰, G. H. Lovell⁴⁹, Y. Lu^{4,b}, C. Lucarelli^{22,j}, D. Lucchesi^{28,o}, S. Luchuk³⁸, M. Lucio Martinez³², V. Lukashenko^{32,46}, Y. Luo³, A. Lupato⁵⁶, E. Luppi^{21,i}, A. Lusiani^{29,q}, K. Lynch¹⁸, X.-R. Lyu⁶, L. Ma⁴, R. Ma⁶, S. Maccolini²⁰, F. Machefert¹¹, F. Maciuc³⁷, V. Macko⁴³, P. Mackowiak¹⁵, S. Maddrell-Mander⁴⁸, L. R. Madhan Mohan⁴⁸, A. Maevskiy³⁸, D. Maisuzenko³⁸, M. W. Majewski³⁴, J. J. Malczewski³⁵, S. Malde⁵⁷, B. Malecki^{35,42}, A. Malinin³⁸, T. Maltsev³⁸, H. Malygina¹⁷, G. Manca^{27,h}, G. Mancinelli¹⁰, D. Manuzzi²⁰, C. A. Manzari⁴⁴, D. Marangotto^{25,l}, J. F. Marchand⁸, U. Marconi²⁰, S. Mariani^{22,j}, C. Marin Benito³⁹, M. Marinangeli⁴³, J. Marks¹⁷, A. M. Marshall⁴⁸, P. J. Marshall⁵⁴, G. Martelli^{71,p}, G. Martellotti³⁰, L. Martinazzoli^{42,m}, M. Martinelli^{26,m}, D. Martinez Santos⁴⁰, F. Martinez Vidal⁴¹, A. Massafferri¹, M. Materok¹⁴, R. Matev⁴², A. Mathad⁴⁴, V. Matiunin³⁸, C. Matteuzzi²⁶, K. R. Mattioli⁷⁶, A. Mauri³², E. Maurice¹², J. Mauricio³⁹, M. Mazurek⁴², M. McCann⁵⁵, L. Mcconnell¹⁸, T. H. McGrath⁵⁶, N. T. McHugh⁵³, A. McNab⁵⁶, R. McNulty¹⁸, J. V. Mead⁵⁴, B. Meadows⁵⁹, G. Meier¹⁵, D. Melnychuk³⁶, S. Meloni^{26,m}, M. Merk^{32,73}, A. Merli^{25,l}, L. Meyer Garcia², D. Miao^{4,6}, M. Mikhasenko^{69,d}, D. A. Milanes⁶⁸, E. Millard⁵⁰, M. Milovanovic⁴², M.-N. Minard^{8,*}, A. Minotti^{26,m}, S. E. Mitchell⁵², B. Mitreska⁵⁶, D. S. Mitzel¹⁵

- A. Mödden¹⁵, R. A. Mohammed⁵⁷, R. D. Moise⁵⁵, S. Mokhnenco³⁸, T. Mombächer⁴⁰, I. A. Monroy⁶⁸, S. Monteil⁹, M. Morandin²⁸, G. Morello²³, M. J. Morello^{29,q}, J. Moron³⁴, A. B. Morris⁶⁹, A. G. Morris⁵⁰, R. Mountain⁶², H. Mu³, F. Muheim⁵², M. Mulder⁷², K. Müller⁴⁴, C. H. Murphy⁵⁷, D. Murray⁵⁶, R. Murta⁵⁵, P. Muzzetto^{27,h}, P. Naik⁴⁸, T. Nakada⁴³, R. Nandakumar⁵¹, T. Nanut⁴², I. Nasteva², M. Needham⁵², N. Neri^{25,l}, S. Neubert⁶⁹, N. Neufeld⁴², P. Neustroev³⁸, R. Newcombe⁵⁵, E. M. Niel⁴³, S. Nieswand¹⁴, N. Nikitin³⁸, N. S. Nolte⁵⁸, C. Normand^{8,h,27}, C. Nunez⁷⁶, A. Oblakowska-Mucha³⁴, V. Obraztsov³⁸, T. Oeser¹⁴, D. P. O'Hanlon⁴⁸, S. Okamura^{21,i}, R. Olderman^{27,h}, F. Oliva⁵², M. E. Olivares⁶², C. J. G. Onderwater⁷², R. H. O'Neil⁵², J. M. Otalora Goicochea², T. Ovsiannikova³⁸, P. Owen⁴⁴, A. Oyanguren⁴¹, O. Ozcelik⁵², K. O. Paddeken⁶⁹, B. Pagare⁵⁰, P. R. Pais⁴², T. Pajero⁵⁷, A. Palano¹⁹, M. Palutan²³, Y. Pan⁵⁶, G. Panshin³⁸, A. Papanestis⁵¹, M. Pappagallo^{19,f}, L. L. Pappalardo^{21,i}, C. Pappenheimer⁵⁹, W. Parker⁶⁰, C. Parkes⁵⁶, B. Passalacqua^{21,i}, G. Passaleva²², A. Pastore¹⁹, M. Patel⁵⁵, C. Patrignani^{20,g}, C. J. Pawley⁷³, A. Pearce⁴², A. Pellegrino³², M. Pepe Altarelli⁴², S. Perazzini²⁰, D. Pereima³⁸, A. Pereiro Castro⁴⁰, P. Perret⁹, M. Petric⁵³, K. Petridis⁴⁸, A. Petrolini^{24,k}, A. Petrov³⁸, S. Petrucci⁵², M. Petruzzo²⁵, H. Pham⁶², A. Philippov³⁸, R. Piandani⁶, L. Pica^{29,q}, M. Piccini⁷¹, B. Pietrzyk⁸, G. Pietrzyk¹¹, M. Pili⁵⁷, D. Pinci³⁰, F. Pisani⁴², M. Pizzichemi^{26,m,42}, V. Placinta³⁷, J. Plews⁴⁷, M. Plo Casasus⁴⁰, F. Polci^{13,42}, M. Poli Lener²³, M. Poliakova⁶², A. Poluektov¹⁰, N. Polukhina³⁸, I. Polyakov⁴², E. Polycarpo², S. Ponce⁴², D. Popov^{6,42}, S. Popov³⁸, S. Poslavskii³⁸, K. Prasanth³⁵, L. Promberger⁴², C. Prouve⁴⁰, V. Pugatch⁴⁶, V. Puill¹¹, G. Punzi^{29,r}, H. R. Qi³, W. Qian⁶, N. Qin³, S. Qu³, R. Quagliani⁴³, N. V. Raab¹⁸, R. I. Rabadan Trejo⁶, B. Rachwal³⁴, J. H. Rademacker⁴⁸, R. Rajagopalan⁶², M. Rama²⁹, M. Ramos Pernas⁵⁰, M. S. Rangel², F. Ratnikov³⁸, G. Raven^{33,42}, M. Rebollo De Miguel⁴¹, F. Redi⁴², F. Reiss⁵⁶, C. Remon Alepuz⁴¹, Z. Ren³, V. Renaudin⁵⁷, P. K. Resmi¹⁰, R. Ribatti^{29,q}, A. M. Ricci²⁷, S. Ricciardi⁵¹, M. Richardson-Slipper⁵², K. Rinnert⁵⁴, P. Robbe¹¹, G. Robertson⁵², A. B. Rodrigues⁴³, E. Rodrigues⁵⁴, J. A. Rodriguez Lopez⁶⁸, E. Rodriguez Rodriguez⁴⁰, A. Rollings⁵⁷, P. Roloff⁴², V. Romanovskiy³⁸, M. Romero Lamas⁴⁰, A. Romero Vidal⁴⁰, J. D. Roth^{76,*}, M. Rotondo²³, M. S. Rudolph⁶², T. Ruf⁴², R. A. Ruiz Fernandez⁴⁰, J. Ruiz Vidal⁴¹, A. Ryzhikov³⁸, J. Ryzka³⁴, J. J. Saborido Silva⁴⁰, N. Sagidova³⁸, N. Sahoo⁴⁷, B. Saitta^{27,h}, M. Salomon⁴², C. Sanchez Gras³², I. Sanderswood⁴¹, R. Santacesaria³⁰, C. Santamarina Rios⁴⁰, M. Santimaria²³, E. Santovetti^{31,t}, D. Saranin³⁸, G. Sarpis¹⁴, M. Sarpis⁶⁹, A. Sarti³⁰, C. Satriano^{30,s}, A. Satta³¹, M. Saur¹⁵, D. Savrina³⁸, H. Sazak⁹, L. G. Scantlebury Smead⁵⁷, A. Scarabotto¹³, S. Schael¹⁴, S. Scherl⁵⁴, M. Schiller⁵³, H. Schindler⁴², M. Schmelling¹⁶, B. Schmidt⁴², S. Schmitt¹⁴, O. Schneider⁴³, A. Schopper⁴², M. Schubiger³², S. Schulte⁴³, M. H. Schune¹¹, R. Schwemmer⁴², B. Sciascia^{23,42}, A. Sciucchiati⁴², S. Sellam⁴⁰, A. Semennikov³⁸, M. Senghi Soares³³, A. Sergi^{24,k}, N. Serra⁴⁴, L. Sestini²⁸, A. Seuthe¹⁵, Y. Shang⁵, D. M. Shangase⁷⁶, M. Shapkin³⁸, I. Shchemberov³⁸, L. Shchutska⁴³, T. Shears⁵⁴, L. Shekhtman³⁸, Z. Shen⁵, S. Sheng^{4,6}, V. Shevchenko³⁸, B. Shi⁶, E. B. Shields^{26,m}, Y. Shimizu¹¹, E. Shmanin³⁸, J. D. Shupperd⁶², B. G. Siddi^{21,i}, R. Silva Coutinho⁴⁴, G. Simi²⁸, S. Simone^{19,f}, M. Singla⁶³, N. Skidmore⁵⁶, R. Skuza¹⁷, T. Skwarnicki⁶², M. W. Slater⁴⁷, J. C. Smallwood⁵⁷, J. G. Smeaton⁴⁹, E. Smith⁴⁴, K. Smith⁶¹, M. Smith⁵⁵, A. Snoch³², L. Soares Lavra⁹, M. D. Sokoloff⁵⁹, F. J. P. Soler⁵³, A. Solomin^{38,48}, A. Solovev³⁸, I. Solovyev³⁸, F. L. Souza De Almeida², B. Souza De Paula², B. Spaan^{15,*}, E. Spadaro Norella^{25,l}, E. Spiridenkov³⁸, P. Spradlin⁵³, V. Sriskaran⁴², F. Stagni⁴², M. Stahl⁵⁹, S. Stahl⁴², S. Stanislaus⁵⁷, E. N. Stein⁴², O. Steinkamp⁴⁴, O. Stenyakin³⁸, H. Stevens¹⁵, S. Stone^{62,*}, D. Strekalina³⁸, F. Suljik⁵⁷, J. Sun²⁷, L. Sun⁶⁷, Y. Sun⁶⁰, P. Svihra⁵⁶, P. N. Swallow⁴⁷, K. Swientek³⁴, A. Szabelski³⁶, T. Szumlak³⁴, M. Szymanski⁴², Y. Tan³, S. Taneja⁵⁶, A. R. Tanner⁴⁸, M. D. Tat⁵⁷, A. Terentev³⁸, F. Teubert⁴², E. Thomas⁴², D. J. D. Thompson⁴⁷, K. A. Thomson⁵⁴, H. Tilquin⁵⁵, V. Tisserand⁹, S. T'Jampens⁸, M. Tobin⁴, L. Tomassetti^{21,i}, G. Tonani^{25,l}, X. Tong⁵, D. Torres Machado¹, D. Y. Tou³, E. Trifonova³⁸, S. M. Trilov⁴⁸, C. Tripli⁴³, G. Tuci⁶, A. Tully⁴³, N. Tuning^{32,42}, A. Ukleja³⁶, D. J. Unverzagt¹⁷, E. Ursov³⁸, A. Usachov³², A. Ustyuzhanin³⁸, U. Uwer¹⁷, A. Vagner³⁸, V. Vagnoni²⁰, A. Valassi⁴², G. Valenti²⁰, N. Valls Canudas⁷⁴, M. van Beuzekom³², M. Van Dijk⁴³, H. Van Hecke⁶¹, E. van Herwijnen³⁸, M. van Veghel⁷², R. Vazquez Gomez³⁹, P. Vazquez Regueiro⁴⁰, C. Vázquez Sierra⁴², S. Vecchi²¹, J. J. Velthuis⁴⁸, M. Veltri^{22,v}, A. Venkateswaran⁶², M. Veronesi³², M. Vesterinen⁵⁰, D. Vieira⁵⁹, M. Vieites Diaz⁴³, X. Vilasis-Cardona⁷⁴, E. Vilella Figueras⁵⁴, A. Villa²⁰, P. Vincent¹³, F. C. Volle¹¹, D. vom Bruch¹⁰, A. Vorobyev³⁸, V. Vorobyev³⁸, N. Voropaev³⁸, K. Vos⁷³, C. Vrahas⁵², R. Waldi¹⁷, J. Walsh²⁹, G. Wan⁵, C. Wang¹⁷, J. Wang⁵, J. Wang⁴, J. Wang³, J. Wang⁶⁷, M. Wang⁵, R. Wang⁴⁸, X. Wang⁶⁶, Y. Wang⁷, Z. Wang⁴⁴, Z. Wang³, Z. Wang⁶, J. A. Ward^{50,63}, N. K. Watson⁴⁷, D. Websdale⁵⁵, Y. Wei⁵

C. Weisser⁵⁸, B. D. C. Westhenry⁴⁸ , D. J. White⁵⁶ , M. Whitehead⁵³ , A. R. Wiederhold⁵⁰ , D. Wiedner¹⁵ , G. Wilkinson⁵⁷ , M. K. Wilkinson⁵⁹ , I. Williams⁴⁹, M. Williams⁵⁸ , M. R. J. Williams⁵² , R. Williams⁴⁹ , F. F. Wilson⁵¹ , W. Wislicki³⁶ , M. Witek³⁵ , L. Witola¹⁷ , C. P. Wong⁶¹ , G. Wormser¹¹ , S. A. Wotton⁴⁹ , H. Wu⁶² , K. Wyllie⁴² , Z. Xiang⁶ , D. Xiao⁷ , Y. Xie⁷ , A. Xu⁵ , J. Xu⁶ , L. Xu³ , M. Xu⁵⁰ , Q. Xu⁶, Z. Xu⁹ , Z. Xu⁶ , D. Yang³ , S. Yang⁶ , Y. Yang⁶ , Z. Yang⁵ , Z. Yang⁶⁰ , L. E. Yeomans⁵⁴ , H. Yin⁷ , J. Yu⁶⁵ , X. Yuan⁶² , E. Zaffaroni⁴³ , M. Zavertyaev¹⁶ , M. Zdybal³⁵ , O. Zenaiev⁴² , M. Zeng³ , D. Zhang⁷ , L. Zhang³ , S. Zhang⁶⁵ , S. Zhang⁵ , Y. Zhang⁵ , Y. Zhang⁵⁷ , A. Zharkova³⁸ , A. Zhelezov¹⁷ , Y. Zheng⁶ , T. Zhou⁵ , X. Zhou⁶ , Y. Zhou⁶ , V. Zhovkovska¹¹ , X. Zhu³ , X. Zhu⁷ , Z. Zhu⁶ , V. Zhukov^{14,38} , Q. Zou^{4,6} , S. Zucchelli^{20,g} , D. Zuliani²⁸ , G. Zunica⁵⁶

¹ Centro Brasileiro de Pesquisas Físicas (CBPF), Rio de Janeiro, Brazil

² Universidade Federal do Rio de Janeiro (UFRJ), Rio de Janeiro, Brazil

³ Center for High Energy Physics, Tsinghua University, Beijing, China

⁴ Institute Of High Energy Physics (IHEP), Beijing, China

⁵ School of Physics State Key Laboratory of Nuclear Physics and Technology, Peking University, Beijing, China

⁶ University of Chinese Academy of Sciences, Beijing, China

⁷ Institute of Particle Physics, Central China Normal University, Wuhan, Hubei, China

⁸ CNRS, IN2P3-LAPP, Université Savoie Mont Blanc, Annecy, France

⁹ CNRS/IN2P3, LPC, Université Clermont Auvergne, Clermont-Ferrand, France

¹⁰ CNRS/IN2P3, CPPM, Aix Marseille Univ, Marseille, France

¹¹ CNRS/IN2P3, IJCLab, Université Paris-Saclay, Orsay, France

¹² Laboratoire Leprince-Ringuet, CNRS/IN2P3, Ecole Polytechnique, Institut Polytechnique de Paris, Palaiseau, France

¹³ LPNHE, CNRS/IN2P3, Sorbonne Université, Paris Diderot Sorbonne Paris Cité, Paris, France

¹⁴ I. Physikalisches Institut, RWTH Aachen University, Aachen, Germany

¹⁵ Fakultät Physik, Technische Universität Dortmund, Dortmund, Germany

¹⁶ Max-Planck-Institut für Kernphysik (MPIK), Heidelberg, Germany

¹⁷ Physikalischs Institut, Ruprecht-Karls-Universität Heidelberg, Heidelberg, Germany

¹⁸ School of Physics, University College Dublin, Dublin, Ireland

¹⁹ INFN Sezione di Bari, Bari, Italy

²⁰ INFN Sezione di Bologna, Bologna, Italy

²¹ INFN Sezione di Ferrara, Ferrara, Italy

²² INFN Sezione di Firenze, Firenze, Italy

²³ INFN Laboratori Nazionali di Frascati, Frascati, Italy

²⁴ INFN Sezione di Genova, Genoa, Italy

²⁵ INFN Sezione di Milano, Milan, Italy

²⁶ INFN Sezione di Milano-Bicocca, Milan, Italy

²⁷ INFN Sezione di Cagliari, Monserrato, Italy

²⁸ Università degli Studi di Padova, Università e INFN, Padova, Padua, Italy

²⁹ INFN Sezione di Pisa, Pisa, Italy

³⁰ INFN Sezione di Roma La Sapienza, Rome, Italy

³¹ INFN Sezione di Roma Tor Vergata, Rome, Italy

³² Nikhef National Institute for Subatomic Physics, Amsterdam, The Netherlands

³³ Nikhef National Institute for Subatomic Physics and VU University Amsterdam, Amsterdam, The Netherlands

³⁴ Faculty of Physics and Applied Computer Science, AGH-University of Science and Technology, Kraków, Poland

³⁵ Henryk Niewodniczanski Institute of Nuclear Physics Polish Academy of Sciences, Kraków, Poland

³⁶ National Center for Nuclear Research (NCBJ), Warsaw, Poland

³⁷ Horia Hulubei National Institute of Physics and Nuclear Engineering, Bucharest-Magurele, Romania

³⁸ Affiliated with an Institute Covered by a Cooperation Agreement with CERN, Geneva, Switzerland

³⁹ ICCUB, Universitat de Barcelona, Barcelona, Spain

⁴⁰ Instituto Galego de Física de Altas Enerxías (IGFAE), Universidade de Santiago de Compostela, Santiago de Compostela, Spain

⁴¹ Instituto de Fisica Corpuscular, Centro Mixto Universidad de Valencia-CSIC, Valencia, Spain

⁴² European Organization for Nuclear Research (CERN), Geneva, Switzerland

- ⁴³ Institute of Physics, Ecole Polytechnique Fédérale de Lausanne (EPFL), Lausanne, Switzerland
⁴⁴ Physik-Institut, Universität Zürich, Zurich, Switzerland
⁴⁵ NSC Kharkiv Institute of Physics and Technology (NSC KIPT), Kharkiv, Ukraine
⁴⁶ Institute for Nuclear Research of the National Academy of Sciences (KINR), Kyiv, Ukraine
⁴⁷ University of Birmingham, Birmingham, UK
⁴⁸ H.H. Wills Physics Laboratory, University of Bristol, Bristol, UK
⁴⁹ Cavendish Laboratory, University of Cambridge, Cambridge, UK
⁵⁰ Department of Physics, University of Warwick, Coventry, UK
⁵¹ STFC Rutherford Appleton Laboratory, Didcot, UK
⁵² School of Physics and Astronomy, University of Edinburgh, Edinburgh, UK
⁵³ School of Physics and Astronomy, University of Glasgow, Glasgow, UK
⁵⁴ Oliver Lodge Laboratory, University of Liverpool, Liverpool, UK
⁵⁵ Imperial College London, London, UK
⁵⁶ Department of Physics and Astronomy, University of Manchester, Manchester, UK
⁵⁷ Department of Physics, University of Oxford, Oxford, UK
⁵⁸ Massachusetts Institute of Technology, Cambridge, MA, USA
⁵⁹ University of Cincinnati, Cincinnati, OH, USA
⁶⁰ University of Maryland, College Park, MD, USA
⁶¹ Los Alamos National Laboratory (LANL), Los Alamos, NM, USA
⁶² Syracuse University, Syracuse, NY, USA
⁶³ School of Physics and Astronomy, Monash University, Melbourne, Australia, associated to ⁵⁰
⁶⁴ Pontifícia Universidade Católica do Rio de Janeiro (PUC-Rio), Rio de Janeiro, Brazil, associated to ²
⁶⁵ Physics and Micro Electronic College, Hunan University, Changsha City, China, associated to ⁷
⁶⁶ Guangdong Provincial Key Laboratory of Nuclear Science, Guangdong-Hong Kong Joint Laboratory of Quantum Matter, Institute of Quantum Matter, South China Normal University, Guangzhou, China, associated to ³
⁶⁷ School of Physics and Technology, Wuhan University, Wuhan, China, associated to ³
⁶⁸ Departamento de Fisica , Universidad Nacional de Colombia, Bogotá, Colombia, associated to ¹³
⁶⁹ Universität Bonn-Helmholtz-Institut für Strahlen und Kernphysik, Bonn, Germany, associated to ¹⁷
⁷⁰ Eotvos Lorand University, Budapest, Hungary, associated to ⁴²
⁷¹ INFN Sezione di Perugia, Perugia, Italy, associated to ²¹
⁷² Van Swinderen Institute, University of Groningen, Groningen, The Netherlands, associated to ³²
⁷³ Universiteit Maastricht, Maastricht, The Netherlands, associated to ³²
⁷⁴ DS4DS, La Salle, Universitat Ramon Llull, Barcelona, Spain, associated to ³⁹
⁷⁵ Department of Physics and Astronomy, Uppsala University, Uppsala, Sweden, associated to ⁵³
⁷⁶ University of Michigan, Ann Arbor, MI, USA, associated to ⁶²
- ^a Universidade Federal do Triângulo Mineiro (UFTM), Uberaba, MG, Brazil
^b Central South U., Changsha, China
^c Hangzhou Institute for Advanced Study, UCAS, Hangzhou, China
^d Excellence Cluster ORIGINS, Munich, Germany
^e Universidad Nacional Autónoma de Honduras, Tegucigalpa, Honduras
^f Università di Bari, Bari, Italy
^g Università di Bologna, Bologna, Italy
^h Università di Cagliari, Cagliari, Italy
ⁱ Università di Ferrara, Ferrara, Italy
^j Università di Firenze, Firenze, Italy
^k Università di Genova, Genoa, Italy
^l Università degli Studi di Milano, Milan, Italy
^m Università di Milano Bicocca, Milan, Italy
ⁿ Università di Modena e Reggio Emilia, Modena, Italy
^o Università di Padova, Padua, Italy
^p Università di Perugia, Perugia, Italy
^q Scuola Normale Superiore, Pisa, Italy

^r Università di Pisa, Pisa, Italy

^s Università della Basilicata, Potenza, Italy

^t Università di Roma Tor Vergata, Rome, Italy

^u Università di Siena, Siena, Italy

^v Università di Urbino, Urbino, Italy

* Deceased